NONDESTRUCTIVE EVALUATION OF METAL MATRIX COMPOSITES

Scott W. Schramm and Isaac Daniel

IIT Research Institute
10 West 35th Street
Chicago, IL 60620

ABSTRACT

The objective of the subject program was to apply nondestructive evaluation (NDE) methods to assess the integrity of FP/Mg composites. The material investigated was ZE41A magnesium alloy reinforced with FP (aluminum oxide) fiber. Twenty-one specimens (three specimens of each of six flawed and three unflawed specimens) were evaluated using ultrasonic scanning, wave propagation velocity, wave attenuation coefficient, and x-ray radiograph inspection techniques. The results for two of the 21 specimens are included herein.

After the NDE inspections were completed, a representative specimen from each of the seven groups was sectioned and micrographs were made for comparison with the NDE records. It was found that ultrasonic scanning using a 15 MHz compression wave, focused transducer operated in the pulse-echo mode generating an analog C-scan gave the best pictorial results. The wave attenuation and wave propagation velocity measurements were found to be consistent with the ultrasonic C-scans, but x-ray radiography was useful only at locations of gross material defects.

INTRODUCTION

Advanced metal-matrix composite materials possess unique mechanical and physical characteristics which make them highly desirable for specific applications. In addition to the advantages afforded by the anisotropic characteristics common to all composite materials, they have many additional advantages. In general, they exhibit high shear strength and shear modulus, high transverse tensile strength, excellent stability over a wide temperature range, good strength

retention, excellent fatigue and creep properties, and high impact strength.

Composite systems that have received the most attention to date are boron/aluminum, borsic/aluminum, and graphite/aluminum.[1] More recently, with the advent of aluminum oxide (FP) fibers in continuous form, systems such as FP/aluminum and FP/magnesium have been introduced. The basic fabrication techniques for FP/magnesium composites have been developed by DuPont; however, there is a need for improvements in the fabrication process. It is, therefore, of great importance to be able, using available NDE methods, to assess the quality of the composite and to characterize all possible types of flaws that may be introduced during fabrication.

The objective of the parent program was to apply NDE methods to assess the integrity of FP/Mg composites. One of the most common and widely accepted NDE methods is ultrasonic inspection.[2] The preferred method of flaw identification is by comparison of pulse information obtained from known flawed and unflawed standard specimens. Appropriate standards, especially in laminated composites, are not always easy to produce and sometimes are not feasible. Alternative pulse processing/identification techniques for ultrasonic inspection, such as frequency and phase shift analysis and adaptive learning techniques, are being developed.[3-7]

SPECIMENS

The material investigated was ZE41A magnesium alloy reinforced with FP (aluminum oxide) fibers. The specimens were coupons 12.7 cm (5 in.) long x 3.8 cm (1.5 in.) wide x 0.6 cm (0.25 in.) thick with a 0.50 fiber volume ratio. The following FP/Mg specimens with and without defects were fabricated:

- Type 1: Three FP/Mg specimens with no intentional flaws
- Type 2: Three FP/Mg specimens with fiber-matrix debonding
- Type 3: Three FP/Mg specimens with porosity
- Type 4: Three FP/Mg specimens with fiber misalignment
- Type 5: Three FP/Mg specimens with fiber fracture
- Type 6: Three FP/Mg specimens with nonuniform fiber distribution
- Type 7: Three FP/Mg specimens with matrix fracture.

NONDESTRUCTIVE EVALUATION METHODS

Throughout the course of the program, a minimum of one specimen from each of the seven specimen types was subjected to all five NDE methods investigated in the program. The five NDE methods used were:

- Ultrasonic inspection, including A-scans, C-scan (conventional pen-lift), and C-scans (analog)

- Ultrasonic attenuation, including contact transducer and water delay line techniques

- Ultrasonic backscattering

- Wave propagation velocity

- X-ray radiography.

Each of these methods is described in detail in the following sections.

Ultrasonic Inspection

A Panametrics pulser-receiver was used to drive transducers of 1, 2.25, 5, 10 and 15 MHz frequency. All the transducers were immersion type, focused transducers; 2.5 cm (1 in.) in diameter for the 1, 2.25 and 5 MHz frequencies and 1.3 cm (0.5 in.) in diameter for the 10 and 15 MHz frequencies, respectively. The requirements for determining the transducer selection were: a standoff distance of at least 5.1 cm (2 in.) to clear hardware associated with specimen mounting; high damping and broad bandwidth to provide resolving power for the detection of subsurface flaws; and a small soundbeam cross-section for good definition of flaw boundaries in the plane of the specimen. The nominal focal length in water of the transducers was 6.4 cm (2.5 in.). The focal spot size was 1.3 cm (0.05 in.), which made it possible to outline the boundary of a flaw in the plane of the specimen to within ±.64 mm (±0.025 in.). The X-Y plotter was a Hewlett-Packard Model 7044A X-y recorder. The X and Y control sensitivities range from 0.25 mV/cm to 5 V/cm. The recorded C-scan could be smaller, equal to or larger than the actual specimen up to a size of 25 cm (10 in.) x 38 cm (15 in.). The X-Y recorder could operate in either the pen-lift or analog mode. In the pen-lift mode the output from the peak detector was channeled through an electronic alarm unit into the pen-lift control of the recorder. The alarm unit was set to trigger the pen-lift whenever the amplitude of the peak detector fell below a prescribed level, indicating a flaw; otherwise, the pen stayed in contact with the paper tracing a line. This gives detailed flaw locations in the plane of the specimen with definite outlines of the flaw boundaries. The analog mode supplements this information by giving a continuous record of the amplitude of the gated pulse. It was obtained by scanning the specimen with the (alarm) unit bypassed. The horizontal and vertical motion of the pen was effected by information fed to the X-Y recorder by displacement transducers used on the scanning drive mechanism. The scanning drive mechanism, like the X-Y recorder, was used in conjunction with the compression wave immersion transducers only.

Ultrasonic Attenuation

The objective of the attenuation measurements was to correlate, if possible, the measured attenuation with the condition of the material being evaluated. Since it was important to make the amplitude measurements in a reliable, quantitative, and reproducible manner, a special specimen holder was fabricated. Absolute measurements of attenuation were difficult because the amplitude of the reflected or transmitted pulse depends not only on material attenuation, but also on the energy dissipation in the coupling between transducer and specimen, and on reflection losses. The specimen holder was designed to minimize ultrasonic wave energy losses associated with the transmission of ultrasound to the water through the back-face of the specimen during immersed ultrasonic inspection. The special specimen holder had a watertight seal which, when immersed in water, formed an air pocket adjacent to the back-face of the specimen. Since the impedance mismatch was greater between FP/Mg and air than between FP/Mg and water, less wave energy was lost through the back-face to the air than would be if the specimen were totally surrounded by water.

A minimum of three measurements were made on one specimen from each of the seven specimen types. The measurements were made using a 15 MHz focused, compression wave, immersion transducer operated in the pulse-echo mode. Figure 1 shows a typical ultrasonic attenuation measurement record (A-scan) and corresponding amplitudes. The amplitudes were determined using a digital voltmeter, variable voltage power supply and a dual beam oscilloscope. The amplitude voltages were determined by using one beam of the oscilloscope as a cursor and moving it with the power supply to pass through the peak of the various pulses. The voltages were read off the digital voltmeter.

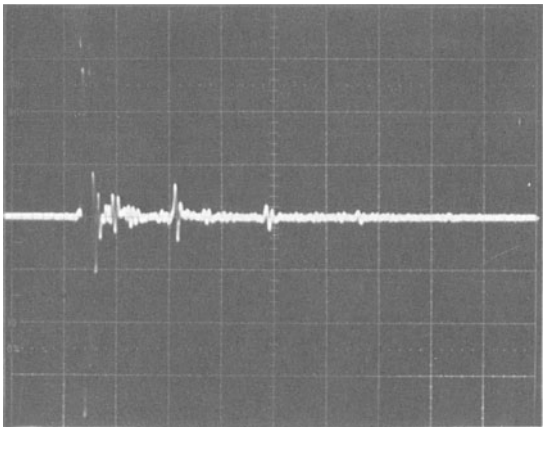

Fig. 1. Ultrasonic attenuation record for FP/Mg specimen without intentional flaws.

A second method of determining the ultrasonic attenuation required the use of a 10 MHz, shear wave, contact transducer operated in the pulse-echo mode. Ultrasonic attenuation records similar to that shown in Fig. 1 were generated and reduced. When the contact transducer was used, propylene glycol ($Z2 = 2.5 \times 10^6$ kg/m^{2}s) was used as an acoustic couplant.

Ultrasonic Backscattering

Ultrasonic backscattering is a technique which utilizes the inhomogeneous, layered nature of the composite to detect and image dominant microstructural features, such as cracks, fibers, etc. The basic concept[8] is that a defect can be identified and possibly characterized from the magnitude and angular distribution of the scattered energy. This can be accomplished by using a device which allows a transducer to be rotated at various surface incident angles. Since the maximum backscattered energy is received by the transmitting/receiving transducer when the transducer is normal to the defect, the shape, location, and orientation of the defect can be determined approximately by angularly indexing the transducer until a maximum reflected signal is generated. The goniometer used provided a full 360° rotation capability and an incident angle variability from 0° to 60°.

Wave Propagation Velocity

The wave propagation velocities were determined using a Panametrics Model 5221 ultrasonic thickness gage. This is equivalent to measuring the wave propagation velocity, since the velocity or travel time must be known to measure the thickness. Any deviation between the thickness measured ultrasonically and that measured directly with a micrometer is related to the difference between the assumed and actual wave propagation velocity.

The longitudinal wave propagation velocities along the three principal material axes of an anisotropic material are given by the usual relations

$$C_{11} = \sqrt{\frac{Q_{11}}{\rho}}$$

$$C_{22} = \sqrt{\frac{Q_{22}}{\rho}}$$

$$C_{33} = \sqrt{\frac{Q_{33}}{\rho}}$$

where Q_{ij} are stiffness and ρ the material density. Any change in propagation velocity is related to changes in modulus and/or density.

X-Ray Radiography

X-ray radiography was done with fine-grained, single emulsion X-ray films. The radiographs were generated using a 62 kV/10 mA excitation energy throughout a 25 sec exposure time. Initially, it was thought that a zinc iodide based penetrant would enhance the radiographic detailing of internal defects; but, the difficulties associated with the preparation and use of the penetrant solution, along with time restrictions, precluded its use. Additionally, the types of defects (adjacent to a free surface or edge) which could be enhanced by the penetrant solution were readily definable by ultrasonic inspection techniques.

TEST PROGRAM

The objective of the program was to apply NDE methods to assess the integrity of FP/Mg composite specimens with various flaw/defect types. Previous program experience[9-11] indicated that of the five NDE methods described in the preceding section, ultrasonic inspection would be the foundation evaluation procedure to which the other procedures would provide supplemental/complementary information.

Again, based on previous program experience, and the inherent acoustic propagation properties of composite laminate specimens, it was assumed that the lower frequency (1 and 2.25 MHz) transducers could be expected to supply very little information on material integrity. After a cursory inspection of several FP/Mg specimens with the 1 and 2.25 MHz transducers operated in the pulse-echo mode, the above assumption was borne out and full surface scanning of the specimens was initiated using a 5 MHz transducer operated in the pulse-echo mode. Results from the 5 MHz inspections indicated that a higher frequency transducer should generate a more detailed C-scan. It was then decided to conduct all subsequent ultrasonic inspections with the 15 MHz transducer, the highest frequency in IITRI's inventory of transducers.

In order not to bias the results of the wave attenuation or wave propagation velocity inspections, preliminary data were taken in a random "blind" procedure. That is, the ultrasonic C-scans were not available to the equipment operator at the time the attenuation or propagation velocity measurements were taken. Only after reduction of the raw data, and a general correlation between C-scan and propagation velocity/attenuation coefficient could be drawn, were measurements taken at locations of "apparent material flaw/damage" as indicated by the C-scans. The term "apparent material flaw/damage" refers to the fact that the true material integrity could not be determined until sectioning and micrographic inspections were completed.

The X-ray radiography and backscattering measurements were taken without regard to the other inspection procedures since they would affect the results of those procedures.

Each of the NDE procedures was applied to all of the specimens sequentially to completion before a different or variation of a procedure was initiated. For example, all the 5 MHz ultrasonic inspections were completed before the wave propagation velocity measurements were started.

RESULTS OF TYPE 3 - POROSITY

Ultrasonic Inspection

Figures 2 and 3 are pen-lift and analog C-scans, respectively, of Specimen 3-1. Both C-scans were generated using a 15 MHz immersion, compression wave transducer operated in the pulse-echo mode with the specimen held in the special fixture. Both C-scans show a well-defined area of apparently flawed material involving approximately 20% of the specimen. The narrow bands of apparent damage running parallel to the fiber direction were identified as surface scratches by A-scan interpretation and visual inspection.

For Specimen 3-1, ultrasonic inspection, pen-lift/analog C-scan and A-scan photographs gave an indication of the presence of an area of porosity involving up to 6 of the 8 plies of the specimen.

Wave Propagation Velocity

Table 1 shows the wave propagation velocities for 20 inspection locations and the average wave propagation velocity of the 20 measurements of Specimen 3-1. The average wave propagation velocity for Specimen 3-1 is within 11% of the theoretical value of 6090 ms^{-1} and within 5% of the empirical average of 6466 ms^{-1} for Specimen 1-1.

Of particular interest for this specimen are the wave velocities at the four inspection locations shown on Figure 2 (3-1-1 through 3-1-4) and inspection location 15 from Table 1. Inspection locations 3-1-1 through 3-1-4 correspond to locations 4, 8, 12, and 16 of Table 1.

Location 15 (from Table 1) shows a disproportionately high wave velocity. This implies the presence of a reflective surface within the thickness which causes an apparent increase in the wave propagation velocity because the ultrasonic thickness gage was set to correspond to a finite micrometer measurement, not the through-the-thickness location of a reflective surface. The magnitude of

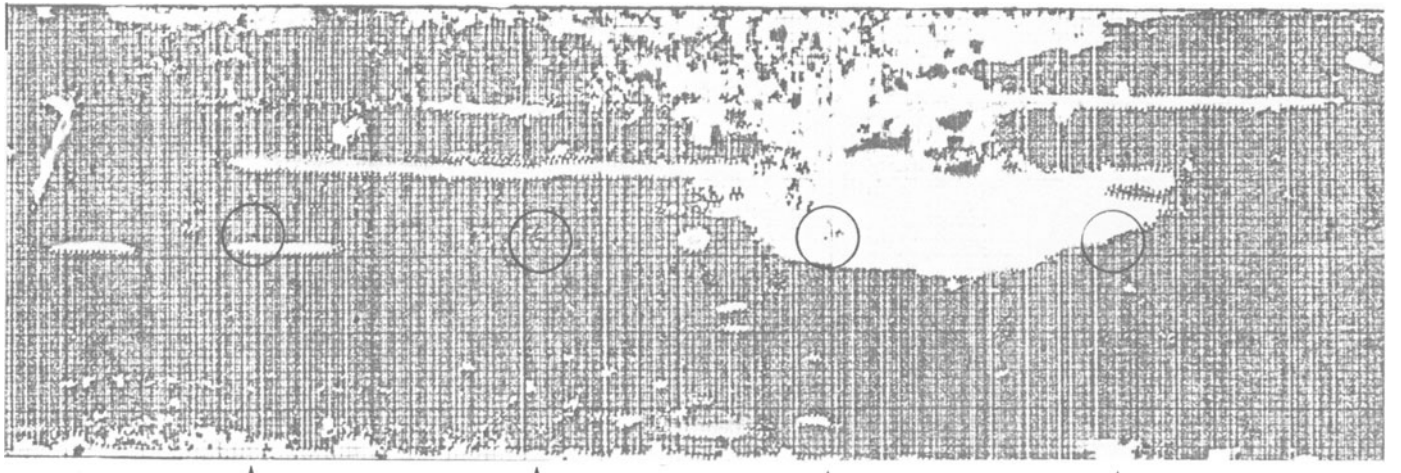

Figure 2. Pen-lift C-scan of FP/Mg Specimen 3-1 (porosity), 15 MHz transducer in pulse-echo mode.

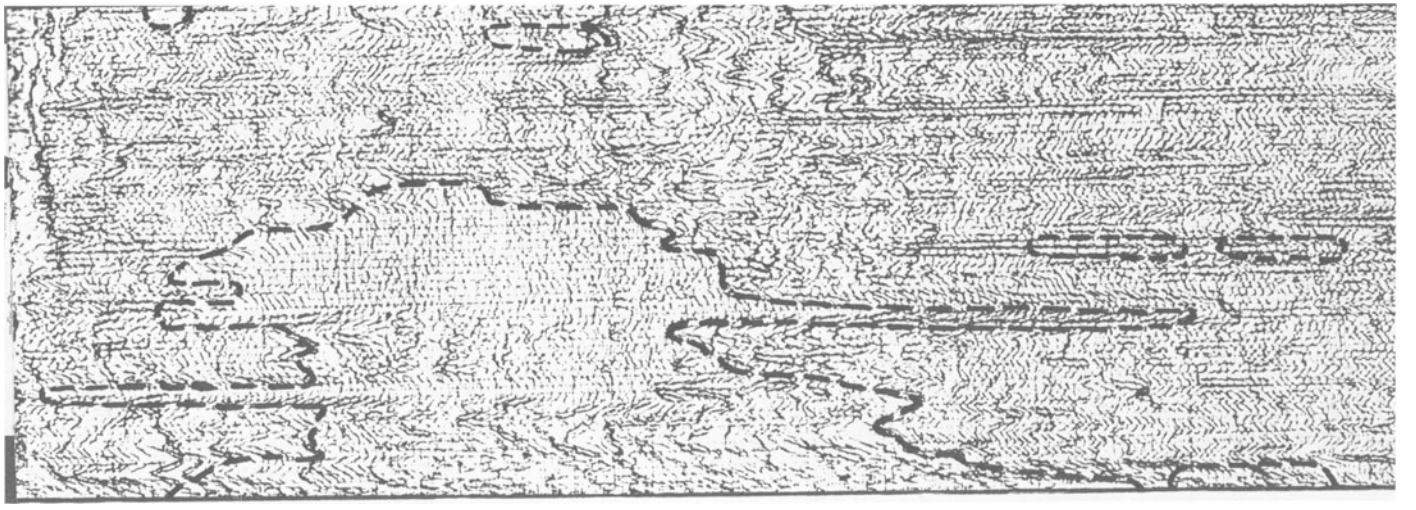

Repetition Rate: 2K Hz
Damping: Variable/Maximum Ohms
Energy: 1
Receiver Attenuation: 6 dB
High Pass Filter: 1.0 MHz
Marked RF: Interface

Gated RF: Medium/Low
Frequency: Less than 8 MHz
Peak Polarity: Negative
Gain: x10
Gain: 40 dB

Figure 3. Analog C-Scan of FP/Mg Specimen 3-1 (porosity), 15 MHz transducer in pulse-echo mode.

TABLE 1. WAVE PROPAGATION VELOCITY ACROSS THE THICKNESS AT VARIOUS LOCATIONS ALONG SPECIMEN CENTERLINE (SPECIMEN 3-1)

Inspection Location	Velocity, ms^{-1} (10^5 in/sec)
1	6610 (2.602)
2	6687 (2.632)
3	6738 (2.652)
4	6679 (2.629)
5	6710 (2.641)
6	6751 (2.657)
7	6761 (2.661)
8	6771 (2.665)
9	6674 (2.627)
10	6522 (2.567)
11	6428 (2.530)
12	6120 (2.409)
13	5943 (2.339)
14	5864 (2.308)
15	10279 (4.046)
16	6723 (2.646)
17	6659 (2.621)
18	6690 (2.633)
19	6702 (2.638)
20	6778 (2.668)
Average	6756 (2.659)

the apparent wave velocity also supports the conclusion that the reflective surface was near the fifth or sixth ply away from the transducer. Based on the average wave propagation velocity of 6570 ms^{-1} (calculated using the 19 values from Table 1, excluding inspection location 15), if the reflective surface was at mid-thickness the apparent wave velocity would be approximately 13,140 ms^{-1}. Correcting for the wave velocity decrease due to the porosity in the travel path before the reflective surface indicates that an apparent wave propagation velocity of 10,279 ms^{-1} would be seen if the reflective surface was 72% into the thickness of the specimen from the front face. For an 8-ply specimen, this corresponds to between the fifth and sixth plies. For Specimen 3-1, wave propagation velocity measurements supported the ultrasonic C-scans and agreed very well with the A-scans as to the extent of the porosity through-the-thickness.

Wave Attenuation

Table 2 shows the wave attenuation coefficients calculated from wave amplitude measurements generated by the water delay line and the contact transducer techniques. the inspection location shown in Table 2 correspond to those shown in Figure 2.

The material attenuation coefficients in Table 2 show good correlation with one another and correspond very well with the C-scans (Figure 2 and 3). Inversely to the wave propagation velocities of the preceding subsection, the maximum attenuation values are seen at inspection location 3-1-3 (inspection area apparently totally flawed), and the minimum attenuation values at inspection location 3-1-2 (inspection are apparently totally unflawed). Again, inspection locations 3-1-1 and 3-1-4 have attenuation values between the extremes of inspection locations 3-1-2 and 3-1-3, which indicated relative percentages of apparent damage.

The material attenuation coefficients calculated for Specimen 3-1 at inspection location 3-1-3 are indicative of the presence of an attenuative defect such as porosity. The nature of the attenuation is due to the impedance mismatch between the FP/Mg material and air pores. This results in a lower ultrasonic wave energy transmission across each succeeding interface; hence, the wave energy rapidly decreases as the wave passes through the specimen.

For Specimen 3-1, the ultrasonic wave attenuation coefficients give an accurate indication as to the presence of a defect such as porosity. The attenuation coefficients correspond very well with the ultrasonic inspection and wave propagation velocity data.

X-Ray Radiography

The radiograph of Specimen 3-1 gave no indication of the presence of the porosity shown by the preceding NDE techniques.

Ultrasonic Backscattering

Ultrasonic backscattering does not appear to be applicable for determination of defects such as porosity. This technique gave no appreciable information as to the state of the material integrity of Specimen 3-1.

Comparison of Inspection Procedures

Of the NDE procedures used to evaluate Specimen 3-1, ultrasonic inspection, wave propagation velocity, and material attenuation coefficients indicated the presence of porosity. Ultrasonic inspection (C-scans with supporting A-scans) gave the most

TABLE 2. ULTRASONIC WAVE ATTENUATION FOR FP/Mg SPECIMEN WITH POROSITY (SPECIMEN 3-1)

Inspection Location	Material Attenuation (α), dB/cm (dB/in)	
	Water Delay Line	Contact Transducer
3-1-1	0.52 (1.32)	0.45 (1.14)
3-1-2	0.44 (1.12)	0.45 (1.14)
3-1-3	0.81 (2.05)	0.76 (1.93)
3-1-4	0.55 (1.39)	0.50 (1.27)

information in that it determined the extent of the area of porosity (by C-scan) and its depth through-the-thickness (by A-scan). Wave propagation measurements corresponded with A-scan information as to the apparent depth through-the-thickness of the porous area and with wave attenuation coefficients as to the dissipative nature of the defect indicating the presence of a porous defect. X-ray radiography and ultrasonic backscattering provided virtually no information as to the state of material integrity of Specimen 3-1.

RESULTS OF TYPE 6 - NONUNIFORM FIBER DISTRIBUTION

Ultrasonic Inspection

Figures 4 and 5 are pen-lift and analog C-scans, respectively, of Specimen 6-2. Both C-scans were generated using a 15 MHz immersion, compression wave transducer operated in the pulse-echo mode with the specimen held in the special fixture. Both the pen-lift and analog C-scan clearly shows the location and extent of the circular area of nonuniform fiber distribution. The circular area is at the mid-length of the specimen. It is towards the left side of the specimen in Figure 4 because the left edge (approximately 20% of the scan length) was inadvertently cropped off before mounting. The additional areas of apparently flawed material on the two C-scans were determined to be surface irregularities by visual inspection and A-scan interpretation.

The Type 6 specimens are unique in that the manufactured flaw is one where only the composition of the material changes as opposed to the material having a physical defect. This is an important distinction because this provides a basis for the determination of the difference between fabrication, quality control discontinuities, and service-related defects.

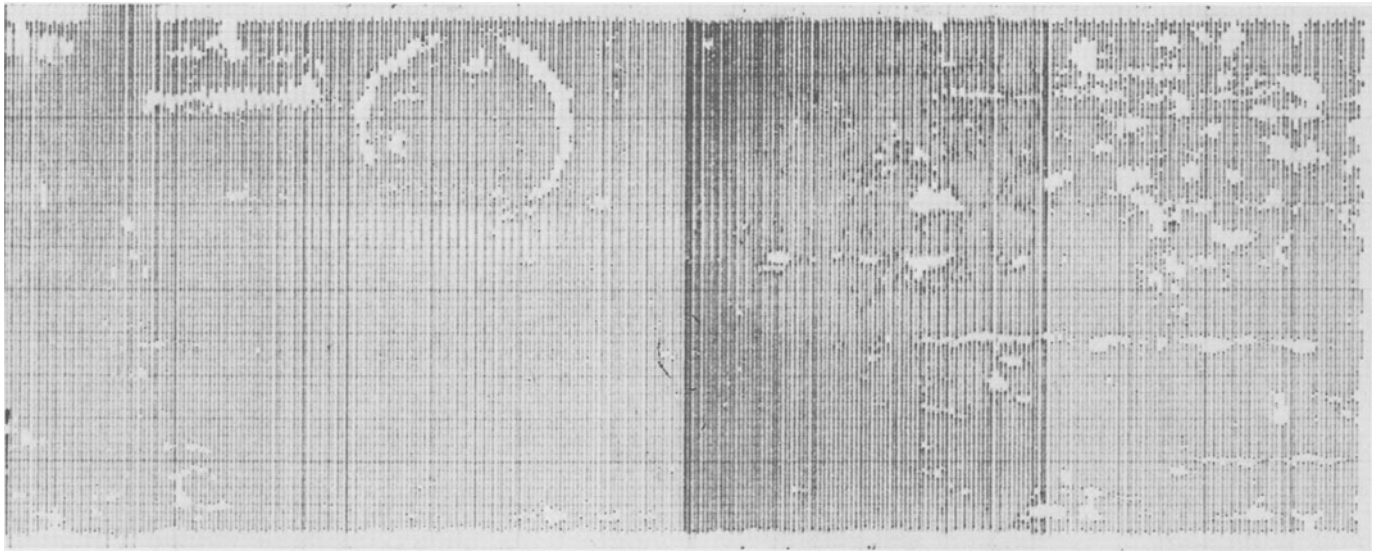

Repetition Rate: 2K Hz
Damping: Variable/Maximum Ohms
Energy: 3
Receiver Attenuation: 6 dB
High Pass Filter: 1.0 MHz
Marked RF: Interface

Gated RF: Medium/Low
Frequency: Greater than 8 MHz
Peak Polarity: Negative
Gain: x10
Gain: 40 dB

Figure 4. Pen-lift C-scan of FP/Mg Specimen 6-2 (nonuniform fiber distribution), 15 MHz transducer in pulse-echo mode.

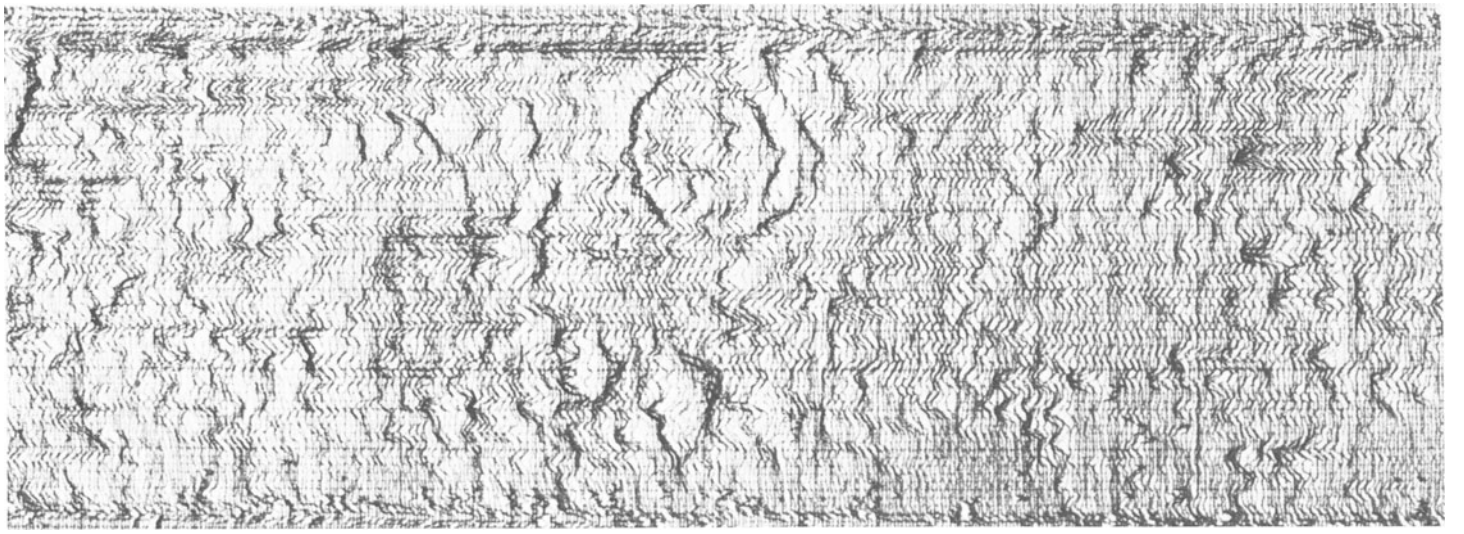

Repetition Rate: 2K Mz
Damping: Variable/Maximum Ohms
Energy: 1
Receiver Attenuation: 6 dB
High Pass Filter: 1.0 MHz
Marked RF: Interface

Gated RF: Medium/Low
Frequency: Greater than 8 MHz
Peak Polarity: Negative
Gain: x10
Gain: 40 dB

Figure 5. Analog C-scan of FP/Mg Specimen 6-2 (nonuniform fiber distribution), 15 MHz transducer in pulse-echo mode.

For Specimen 6-2, ultrasonic inspection gives a representative indication as to the presence and definition of areas of nonuniform fiber distribution.

Wave Propagation Velocity

Figure 6 shows the inspection locations on Specimen 6-2 where wave propagation velocity measurements were taken. Table 3 shows the wave propagation velocities for the 14 inspection locations shown in Figure 6 and the average wave propagation velocity of the first nine measurements. The average wave propagation velocity for Specimen 6-2 (for the unflawed locations) is within 6% of the theoretical value of 6119 ms^{-1} and within 1% of the empirical average of 6466 ms^{-1} for Specimen 1-1. As a comparison, the average wave propagation velocity for 20 inspection locations for Specimen 6-1 was 6466 ms^{-1} which is identical to the empirical average for Specimen 1-1.

The wave propagation velocities for the five inspection locations (6-2-10 through 6-2-14) within the area of nonuniform fiber distribution as indicated by the C-scans (Figures 4 and 5) show a moderate decrease from that within the areas of no apparent material defect. The decrease of the wave propagation is a direct function of the change in composition of the material in that area.

TABLE 3. WAVE PROPAGATION VELOCITY ACROSS THE THICKNESS AT VARIOUS LOCATIONS ALONG SPECIMEN CENTERLINE (SPECIMEN 6-2)

Inspection Location	Velocity, ms^{-1} (10^5 in/sec)
6-2-1	6499 (2.558)
6-2-2	6443 (2.536)
6-2-3	6469 (2.546)
6-2-4	6410 (2.523)
6-2-5	6433 (2.532)
6-2-6	6468 (2.546)
6-2-7	6443 (2.536)
6-2-8	6471 (2.547)
6-2-9	6484 (2.552)
6-2-10	6250 (2.460)
6-2-11	6263 (2.465)
6-2-12	6293 (2.477)
6-2-13	6260 (2.464)
6-2-14	6275 (2.470)
Average 6-2-1 to 6-2-9	6458 (2.542)
Average 6-2-10 to 6-2-14	6268 (2.467)

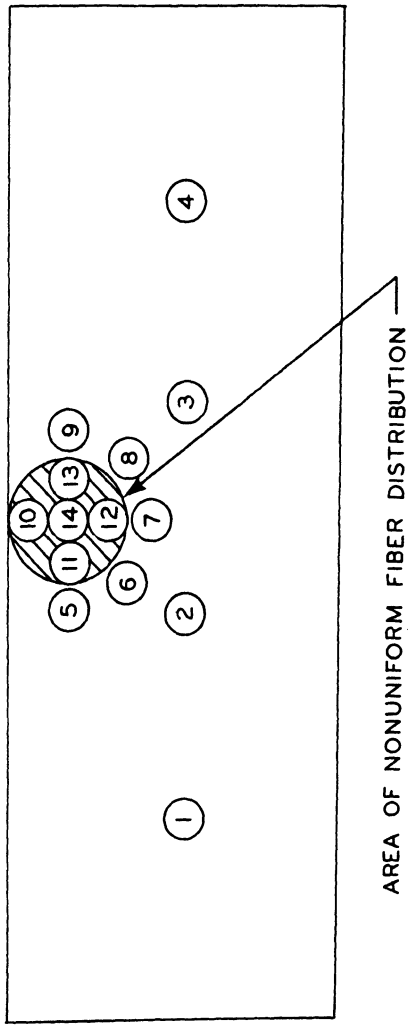

Figure 6. Wave propagation velocity inspection locations for FP/Mg Specimen 6-2 (nonuniform fiber distribution).

The theoretical value of the average wave propagation velocity is nearly identical to the measured average wave propagation velocity for the area of nonuniform fiber distribution for Specimen 6-2 and wave propagation velocity values give a clear indication of the presence of an area of nonuniform fiber distribution.

Wave Attenuation

Table 4 shows the material attenuation coefficients calculated for Specimen 6-2 from measurements taken using the water delay line and contact transducer techniques. The inspection locations indicated in Table 4 correspond to those shown on Figure 6.

The material attenuation coefficients for inspection locations 6-2-1 through 6-2-4 show good agreement with one another for the water delay line technique, but not so for the contact transducer technique. This is explained by the fact that the surface of the specimen was very irregular (as shown in the C-scans, see Figures 4 and 5); hence, the measurements taken with the contact transducer were not as reproducible for Specimen 6-2 as the preceding specimens.

The material attenuation coefficient at inspection location 6-2-14 (within the area of nonuniform fiber distribution) is appreciably higher than those indicated for the other locations. This would be expected at an area of nonuniform fiber distribution because that type of defect causes a decrease in both local density and local modulus which increases the material wave attenuation coefficient. For specimen 6-2, wave attenuation coefficients give an indication of the presence of nonuniform fiber distribution.

X-Ray Radiography

The circular area of nonuniform fiber distribution can be faintly seen in the original radiograph. An enhancement medium would not improve the quality of the radiograph since the defect is neither free surface attached (which provides a flow path for the medium), or the type of defect into which the medium could flow if it were free surface attached. For Specimen 6-2, X-ray radiography gives a faint indication of the presence of an area of nonuniform fiber distribution.

Ultrasonic Backscattering

The backscatter curve gives no indication of the presence of an area of nonuniform fiber distribution beyond the decrease of the amplitude of the reflected pulse. The only activity on the curve occurs when the transducer focal axis sweeps near and through the plane normal to the fiber orientation. For Specimen

TABLE 4. ULTRASONIC WAVE ATTENUATION COEFFICIENTS (SPECIMEN 6-2)

Inspection Location	Water Delay Line	Contact Transducer	Specimen Thickness d_1, cm (in.)	Material Attenuation (α), dB/cm (dB/in.)	
				Water Delay Line	Contact Transducer
6-2-1	0.291	0.242	0.62 (0.243)	0.47 (1.19)	0.39 (0.99)
6-2-2	0.273	0.291	0.62 (0.243)	0.44 (1.11)	0.47 (1.20)
6-2-3	0.273	0.329	0.62 (0.243)	0.44 (1.11)	0.53 (1.35)
6-2-4	0.293	0.256	0.61 (0.240)	0.48 (1.21)	0.42 (1.06)
6-2-14	0.477	0.335	0.62 (0.243)	0.77 (1.97)	0.54 (1.37)

6-2, ultrasonic backscattering does not appear to give any appreciable indication of the presence of an area of nonuniform fiber distribution.

Comparison of Inspection Procedures

Of the NDE procedures used to evaluate Specimen 6-2, ultrasonic inspection, wave propagation velocity, wave attenuation, and X-ray radiography indicated the presence of an area of nonuniform fiber distribution. Both C-scan types showed the locations and extent of the flawed area and interpretation of the A-scans yielded important information about the through-the-thickness position and attenuative nature of the flawed area. Wave propagation velocity data and calculated material attenuation coefficients agreed very well with the C-scans and ultrasonic attenuation theory in differentiating unflawed from flawed areas of the specimen. X-ray radiography showed that the shape and extent of the area of nonuniform fiber distribution could be determined by a method other than ultrasonic inspection. Ultrasonic backscattering provided virtually no information as to the state of material integrity of Specimen 6-2.

SUMMARY OF RESULTS

Table 5 summarizes the results presented in the preceding subsections. The ultrasonic inspection and wave propagation velocity techniques were more widely applicable to different flaw types than were the wave attenuation, X-ray radiography, and ultrasonic backscattering techniques. The only flaw type which ultrasonic inspection or wave propagation velocity could not detect was the misaligned fibers, a defect which only ultrasonic backscattering could determine. Since ultrasonic inspection is the only technique which gives a pictorial representation (C-scans) of the material flaw pattern within a specimen, and since it was applicable to the most flaw types, it is the conclusion of this investigation that the ultrasonic inspection technique is the best of the NDE techniques evaluated for determining the material integrity of FP/Mg composites. It is also concluded that amplitude-time records (A-scans), wave propagation velocities, and wave attenuation coefficients provide valuable information about the through-the-thickness characteristics and physical nature of flaws detected by ultrasonic inspection. It is apparent from the data generated during this program that no single NDE technique evaluated can provide all the information required to adequately define the state of material integrity of FP/Mg composites.

Based on the results and conclusions of this investigation, it is recommended that additional work be conducted in evaluating the applicability of NDE to metal matrix composites. Suggestions

TABLE 5. SUMMARY OF RESULTS ON NDE TECHNIQUES FOR DETECTION OF FLAWS

Specimen	Ultrasonic Inspection C-Scan Pen-Lift	Ultrasonic Inspection C-Scan Analog	Ultrasonic Inspection A-Scan	Wave Propagation	Wave Attenuation Water Delay Line	Wave Attenuation Contact Transducer	X-Ray Radiography Unenhanced	X-Ray Radiography Enhanced	Ultrasonic Backscattering
1-1	OK	OK	OK	OK	OK	OK	OK	OK	OK
2-1	Y	Y	Y	Y	N	N	Y	P	N
3-1	Y	Y	Y	Y	Y	Y	N	P	N
4-1	N	N	N	N	N	N	N	P	Y
5-1	N (P)	Y	Y	Y	Y	Y	N	P	N
6-2	Y	Y	Y	Y	Y	Y	Y	N	N
7-2	Y	Y	Y	Y	Y	Y	Y	P	N

OK - Show further applicability of the inspection technique based on the results of inspection of Specimen 1-1.

Y - Provided a positive indication of the presence of the flaw type in the specimen indicated.

N - Did not provide any indication of the presence of the flaw type in the specimen indicated.

P - Indicates that an equipment or procedure change may make the inspection applicable for the detection of the flaw type in the specimen indicated.

for additional work include the use of higher frequency (greater than 15 MHz) transducers in ultrasonic inspection or frequency distribution analyses. Also, it is recommended that NDE be applied to FP/Mg specimens subjected to an "in service" simulation of applied loads. This type of investigation would indicate which NDE techniques could map increases in flaw size as a function of load application.

SUMMARY AND CONCLUSIONS

The objective of this program was to apply NDE methods to assess the integrity of FP/magnesium composites. The program was performed using an existing ultrasonic detection and recording system using compression wave transducers operated in the pulse-echo mode at five frequencies of 1, 2.25, 5, 10, and 15 MHz. Additionally, low energy X-ray radiography was done with a commercially available X-ray unit.

It was found that ultrasonic inspection with a 15 MHz transducer generating an analog C-scan gave the best pictorial representation of the presence of a majority of the flaw types investigated. Pen-lift C-scans were comparable to analog C-scans for most of the flaw types investigated and, where they were not comparable, an increase in transducer frequency could be expected to make them comparable to the analog C-scans. A-scans, wave propagation velocities, and wave attenuation coefficients corresponded very well with the C-scans, but since they are point inspection procedures, they are difficult to use to map the extent of flaws. Unenhanced X-ray radiography was applicable to approximately half of the flaw types investigated, and indications are that the use of enhancement media would considerably increase the applicability of X-ray radiography. Although used only cursorily, ultrasonic backscattering gave little indication of applicability to more than one specific flaw type.

An encouraging result of this program is that although the FP/Mg composite is a relatively sophisticated material to fabricate and use, its integrity can be determined without using exotic inspection techniques or equipment. This is impressive in the light of the number of specimens and number of flaw types investigated.

ACKNOWLEDGEMENT

The parent program, "Nondestructive Evaluation of Metal-Matrix Composites," from which the data for this paper was drawn, was sponsored by the Army Materials and Mechanics Research Center, Watertown, Massachusetts. Mr. John Nunes was the technical monitor throughout the course of the program.

REFERENCES

1. "Hybrid and Select Metal Matrix Composites," W.J. Renton (ed.), American Institute of Aeronautics and Astronautics, New York, NY, 1977.
2. R.C. McMaster (ed.), "The Nondestructive Testing Handbook," Ronald Press, New York, 1963.
3. J.L. Rose, J.M. Carson and D.J. Leidel, Ultrasonic Procedures for Inspecting Composite Tubes, "Analysis of the Test Methods for High Modulus Fibers and Composites," ASTM STP 521, 311-325, 1973.
4. O.R. Gericke, Ultrasonic Spectroscopy, "Research Techniques in Nondestructive Testing," R.S. Sharpe (ed.), Academic Press, New York, 31-61, 1970.
5. F.H. Chang, R.A. Kline and J.R. Bell, Ultrasonic Evaluation of Adhesive Bond Strength Using Spectroscopic Techniques, General Dynamics, Fort Worth Division, Proceedings of the ARPA/AFML Review of Progress in Quantitative NDe, Scripps Institution of Oceanography, La Jolla, CA, July 18-21, 1978.
6. Interdisciplinary Program for Quantitative Flaw Detection, Rockwell International Science Center, Contract No. F33615-74-C-5180, for ARPA/AFML, September 1975.
7. A.N. Mucciardi, et al., Adaptive Nonlinear Signal Processing for Characterization of Ultrasonic NDE Waveforms, Task 2, Measurements of Subsurface Fatigue Crack Size, Technical Report AFML-TR-76-44, April 1976.
8. Y. Bar-Cohen and R.L. Crane, Nondestructive Evaluation of Fiber-Reinforced Composites with Backscattering Measurements.
9. Advanced Composite Serviceability Program, IIT Research Institute subcontract to Rockwell Internation, Air Force Materials and Flight Dynamics Laboratories, Contract No. F33615-76-C-5344.

10. Test System for Conducting Biaxial Test of Composite Laminates, Air Force Flight Dynamics Laboratories, Contract No. F33615-77-3014.
11. Sensitivity of Ultrasonic Detection of Delaminations and Disbonds in Composite Laminates and Joints, David W. Taylor Naval Ship R&D Center, Contract No. N00167-78-C0085.